Artificial Photosynthetic Reaction Center with a Coumarin-Based Antenna System

ARTICLE *in* THE JOURNAL OF PHYSICAL CHEMISTRY B · MARCH 2013

Impact Factor: 3.3 · DOI: 10.1021/jp402265e · Source: PubMed

7 AUTHORS, INCLUDING:

Gerdenis Kodis
Arizona State University
75 PUBLICATIONS **2,388** CITATIONS
SEE PROFILE

Thomas A Moore
Arizona State University
330 PUBLICATIONS **16,617** CITATIONS
SEE PROFILE

THE JOURNAL OF PHYSICAL CHEMISTRY B

Article

pubs.acs.org/JPCB

Artificial Photosynthetic Reaction Center with a Coumarin-Based Antenna System

Vikas Garg, Gerdenis Kodis, Paul A. Liddell, Yuichi Terazono, Thomas A. Moore,* Ana L. Moore,* and Devens Gust*

Department of Chemistry and Biochemistry, Center for Bio-Inspired Solar Fuel Production, Arizona State University, Tempe, Arizona 85287-1604, United States

Supporting Information

ABSTRACT: In photosynthesis, sunlight is absorbed mainly by antenna chromophores that transfer singlet excitation energy to reaction centers for conversion to useful electrochemical energy. Antennas may likewise be useful in artificial photosynthetic systems that use sunlight to make fuels or electricity. Here, we report the synthesis and spectroscopic properties of a molecular hexad comprising two porphyrin moieties and four coumarin antenna chromophores, all organized by a central hexaphenylbenzene core. Light absorbed by any of the coumarins is transferred to a porphyrin on the 1−10 ps time scale, depending on the site of initial excitation. The quantum yield of singlet energy transfer is 1.0. The energy transfer rate constants are consistent with transfer by the Förster dipole−dipole mechanism. A pyridyl-bearing fullerene moiety self-assembles to the form of the hexad containing zinc porphyrins to yield an antenna−reaction center complex. In the resulting heptad, energy transfer to the porphyrins is followed by photoinduced electron transfer to the fullerene with a time constant of 3 ps. The resulting $P^{\bullet+}-C_{60}^{\bullet-}$ charge-separated state is formed with an overall quantum yield of 1.0 and decays with a time constant of 230 ps in 1,2-difluorobenzene as the solvent.

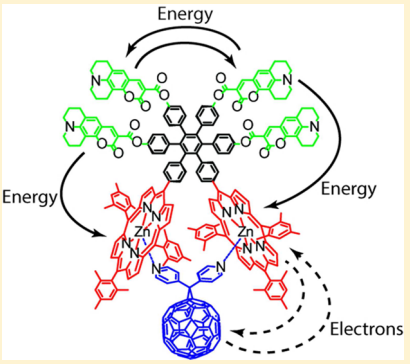

INTRODUCTION

Photosynthetic reaction centers are well-known as the site where excitation energy from sunlight is converted to electrochemical energy via photoinduced electron transfer. However, most photosynthetic light is actually absorbed by antenna systems. The antennas transfer singlet excitation energy spatially within the photosynthetic membranes and ultimately to reaction centers. Organisms contain sufficient antenna chromophores so that they can collect enough light to drive the chemistry at the reaction centers at a useful rate even in dim light. Photosynthetic antennas also carry out photoprotective functions such as non-photochemical quenching[1−5] that help defend the organism from photodamage, especially at high light levels. Chlorophylls are important chromophores in the antenna systems of many organisms, but other pigments play crucial roles. This is because chlorophylls do not absorb light uniformly across the solar spectrum, and at some wavelengths, their extinction coefficients are near zero. Typical auxiliary chromophores include carotenoid polyenes and phycobilins. Carotenoid molecules are particularly important, as they absorb strongly in the 420−500 nm region and they play roles as both antenna chromophores and photoprotective agents.[6−9]

It is likely that antenna systems may also be important components of artificial photosynthetic systems for solar fuel production. As with natural photosynthesis, antennas may be needed in order to efficiently absorb light throughout the part of the solar spectrum that is useful for performing the redox reactions of fuel production. The use of multiple relatively inexpensive antenna molecules to provide excitation energy for more complex and expensive artificial reaction centers[10−14] may be desirable. In addition, artificial antennas could provide photoprotection and photoregulation in order to increase the durability of the system. A large variety of artificial antenna systems has been reported, most of which are based on cyclic tetrapyrrole chromophores.[15−33] In previous work, we have reported the use of non-porphyrinoid antenna chromophores such as bis(phenylethynyl)anthracene and borondipyrromethene as antennas for porphyrin-based artificial photosynthetic reaction centers.[34−36] Other researchers have reported antenna systems based on dyes such as Oregon green and rhodamine red,[37] boron dipyrromethenes,[38] pyrenes and cyanine dyes,[39,40] coumarins,[41] phenylene vinylene polymers,[42] ruthenium complexes,[43] and quantum dots[44,45] bound to various sorts of energy acceptor moieties.

In the present work, we report on the use of a common fluorescent dye, coumarin 343, in an antenna system for a porphyrin−fullerene charge separation unit. This chromophore absorbs in a spectral region similar to that where natural carotenoid antennas absorb, but its photophysical properties

Special Issue: Rienk van Grondelle Festschrift

Received: March 5, 2013
Revised: March 26, 2013

dx.doi.org/10.1021/jp402265e | J. Phys. Chem. B XXXX, XXX, XXX−XXX

are much more suitable for singlet−singlet energy transfer to another molecule. The lifetime of its first excited singlet state is on the time scale of several ns (compared to ca. 10 ps for carotenoids), and it has a high quantum yield of fluorescence, whereas those of the carotenoid are near zero. These properties are favorable for singlet−singlet energy transfer by the Förster mechanism. In antenna complex **1** (Figure 1), the experiments

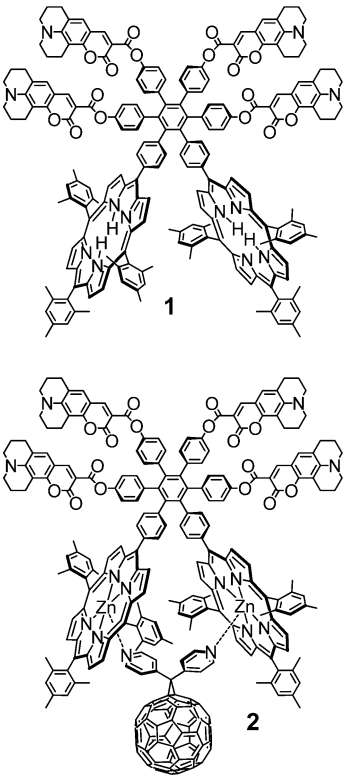

Figure 1. Structures of hexad antenna system **1** and heptad antenna−reaction center **2**. In **2**, the nitrogen atoms of the two pyridine substituents of the fullerene coordinate to the zinc atoms of the two porphyrin moieties.

discussed below show that the four coumarin moieties transfer excitation energy to the porphyrins with a quantum yield near 1.0. Addition of a fullerene electron acceptor by self-assembly through coordination with the zinc atoms of the porphyrins gave artificial antenna−reaction center complex **2**, which demonstrates photoinduced electron transfer from the excited porphyrins to the fullerene with a quantum yield of unity.

RESULTS

Synthesis. In antenna **1**, the various chromophores are organized by a hexaphenylbenzene core. This scaffold is structurally relatively rigid, and the six peripheral phenyl rings are forced to be nearly perpendicular to the central ring by steric interactions. This twisting greatly reduces conjugative interactions between rings. Antenna **1** was prepared as shown in Figure 2 (all synthetic details and compound characterization are reported in the Supporting Information). The hexaphenylbenzene core **5** was synthesized in 86% yield by the Diels−Alder reaction of porphyrin-bearing diarylacetylene **3** with tetraarylcyclopentadienone **4**, followed by loss of carbon monoxide. Acetylene **3** was assembled from porphyrin precursors using palladium-catalyzed coupling reactions.[46] Tetraarylcyclopentadienone **4** was synthesized by the base-

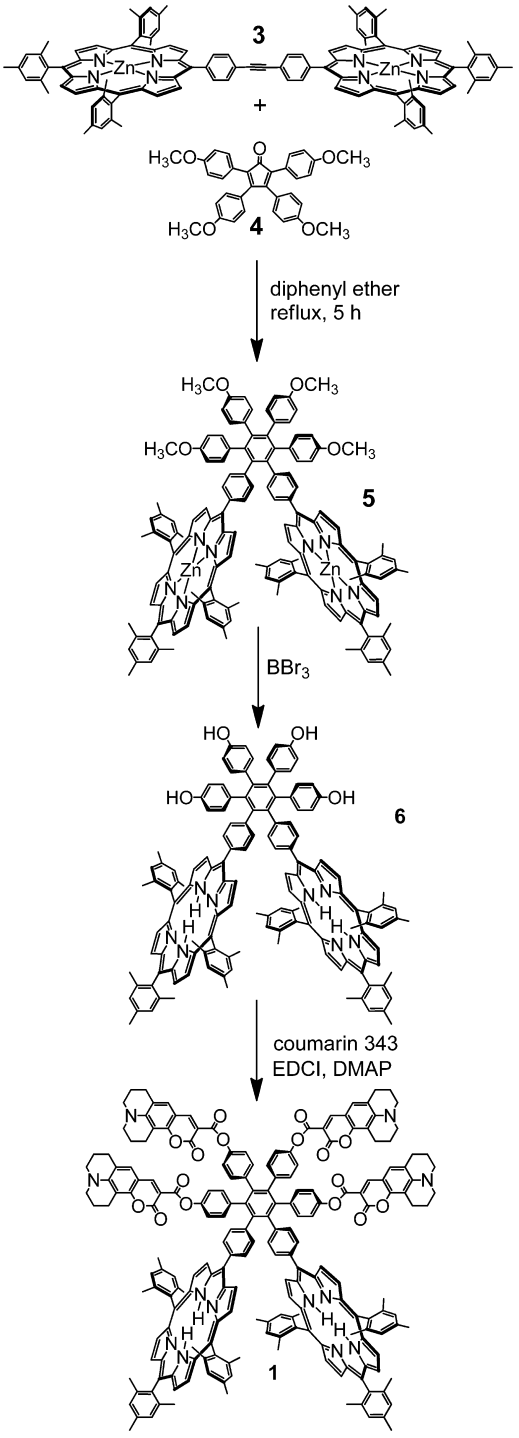

Figure 2. Synthetic route for the preparation of hexad **1**.

catalyzed condensation of a properly substituted dibenzylketone with a properly substituted benzil. The methoxy groups of **5** were cleaved with BBr_3 to yield tetraphenol **6**, which was linked to four coumarin 343 moieties using 1-ethyl-3-(3-dimethylaminopropyl)carbodiimide (EDCI) and 4-dimethylaminopyridine (DMAP) as coupling agents, giving hexad **1** in 90% yield. Heptad **2** was prepared by synthesis of the zinc analogue of **1** followed by self-assembly with fullerene **7**. In addition to **1** and **2**, model compounds **7**−**15** (Figure 3) were prepared in order to help us sort out the complex photochemistry of these molecules. The synthetic methods for **2** and

dx.doi.org/10.1021/jp402265e | J. Phys. Chem. B XXXX, XXX, XXX−XXX

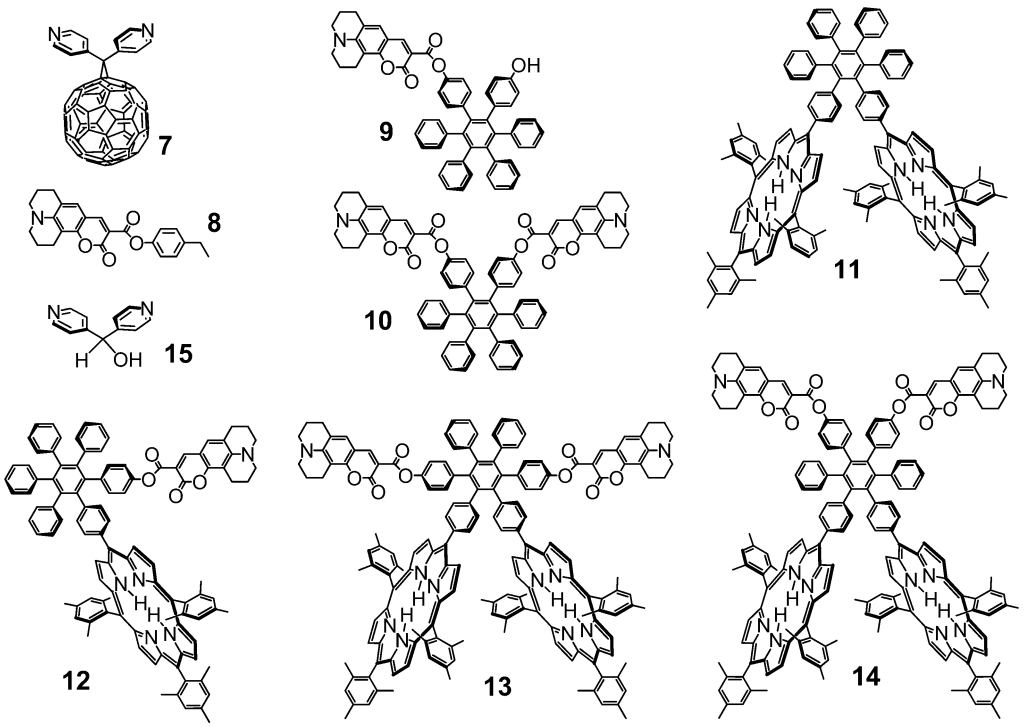

Figure 3. Structures of model compounds synthesized and used in this study.

the model compounds are similar to those used for **1**, and are related in the Supporting Information.

Absorption and Emission Properties of Hexad 1 and Model Compounds. Spectroscopic studies of **1** and related model compounds were carried out in 2-methyltetrahydrofuran solution at ambient temperatures. Figure 4 shows the

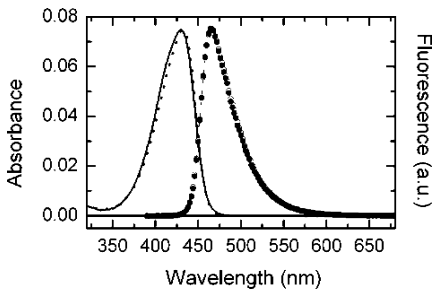

Figure 4. Absorption (lines) and fluorescence emission (circles) spectra of coumarin **9** (dotted line, solid circles) and coumarin dyad **10** (solid line, hollow circles) in 2-methyltetrahydrofuran.

absorption spectra of coumarin model compounds **9** and **10**. Absorption maxima are observed at 432 and 430 nm for **9** and **10**, respectively. Model coumarin **8** has its absorption maximum at 438 nm. These maxima are very close to that of coumarin 343 itself. Fluorescence emission spectra of **9** and **10** are also shown in Figure 4. The emission spectra are nearly mirror images of the absorption spectra, and both have maxima at 465 nm. The fluorescence quantum yield of **8** in 2-methyltetrahydrofuran is 0.78, as determined by comparison to a known standard. These results indicate that the absorption properties of the coumarin moieties are not significantly perturbed either by linkage to the hexaphenylbenzene system or by interactions between the two coumarins. The only indications of intercoumarin interactions are the very slight broadening of the absorption band of the coumarin dyad **10** relative to that of **9** and the small shift of the absorption maxima.

Figure 5 shows spectra from the porphyrin-containing molecules **1**, **11**, **13**, and **14** along with the spectrum of **10**

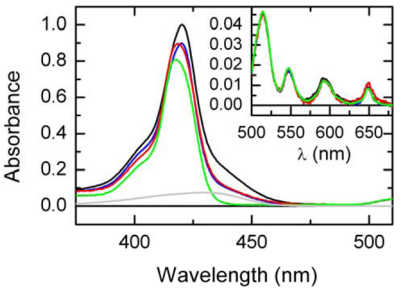

Figure 5. Absorption spectra in 2-methyltetrahydrofuran of hexad **1** (black), tetrad **14** (red), tetrad **13** (blue), porphyrin dyad **11** (green), and coumarin dyad **10** (gray). The absorption spectra of the porphyrin materials were normalized at the 515 nm Q-band. The inset shows the Q-band region for the porphyrin-containing compounds.

for reference. Looking first at the spectrum of porphyrin dyad **11**, we find a Soret maximum at 418 nm and Q-band absorptions at 515, 547, 594, and 649 nm. These characteristics are typical for free base tetraarylporphyrins. The Soret absorption shows a slight broadening due to excitonic splitting that arises from the close approach of the two porphyrin moieties. Such splitting has been seen in related molecules.[36] The spectrum of tetrad **14**, which features two porphyrins and two coumarins in positions *meta* to the nearest porphyrins (relative to the central ring of the hexaphenylbenzene), has a Soret maximum at 418.5 nm. This small apparent shift relative to **11** is likely due to the effect of the underlying coumarin absorption (see spectrum of **10**) and in any case shows that the

dx.doi.org/10.1021/jp402265e | J. Phys. Chem. B XXXX, XXX, XXX−XXX

coumarins cause essentially no perturbations of the porphyrin absorptions. The Q-bands of **14** are identical to those of **11**. In tetrad **13**, in which the coumarins are *ortho* to their porphyrin nearest neighbors, the Q-band positions are unchanged, but the Soret now appears at 420 nm. This ca. 2 nm shift to longer wavelengths indicates a stronger interaction between the porphyrins and coumarin antennas than in **14**, although the perturbation is still minor. Hexad **1** also shows this interaction, with the Soret at 420 nm, and the Q-band positions are identical to those of the other compounds. The increase in the extinction coefficient in the Soret region for the various porphyrin−coumarin combinations relative to that of **11** is due to the underlying broad coumarin absorption (see also Figure 4). All of these porphyrin-containing compounds demonstrate fluorescence emission, with maxima at ca. 651 and 721 nm.

Fluorescence Excitation Spectra. In order to determine whether light absorbed by the coumarin moieties leads to singlet−singlet energy transfer to the porphyrins, the fluorescence excitation spectrum of hexad **1** was obtained in 2-methyltetrahydrofuran (A < 0.05 at all wavelengths, Figure 6). This spectrum was obtained by monitoring the fluorescence

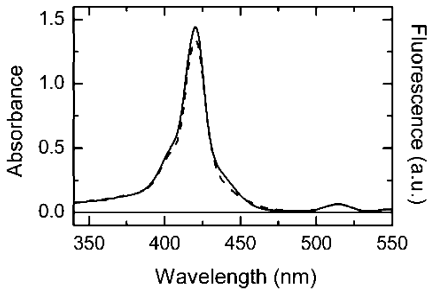

Figure 6. Absorption (solid line) and corrected fluorescence excitation (dashed line) spectra of hexad **1** monitored at 720 nm in 2-methyltetrahydrofuran. The spectra have been normalized at 649 nm where the coumarin moieties do not absorb.

emission at 720 nm as a function of excitation wavelength. The excitation spectrum was corrected for the lamp and monochromator characteristics as a function of wavelength, and was normalized to the absorption spectrum at 649 nm, where the coumarin does not absorb. The excitation and absorption spectra are nearly superimposable, even in the region from about 430 to 460 nm where most of the absorption is due to the coumarin. This shows that the energy transfer efficiency is very high. Quantitatively, the energy transfer efficiency is calculated to be ca. 93% from this plot. Thus, the coumarins are indeed excellent antennas for the porphyrins.

Time-Resolved Fluorescence Studies. In order to learn more about the energy transfer process, time-resolved fluorescence studies were performed using the single photon timing technique. Coumarin model compound **9** in 2-methyltetrahydrofuran was excited at 300 nm and fluorescence was monitored at 490 nm. The coumarin moiety absorbs at this wavelength, although the spectrum is not shown in Figure 4. The decay was fitted as a single exponential process with a time constant of 2.7 ns (χ^2 = 1.12). A similar experiment with dicoumarin **10** yielded a lifetime of 2.4 ns (χ^2 = 1.13). Thus, the *ortho* arrangement of the two coumarin moieties in **10** does not result in any interchromophore interactions that significantly change the lifetime of the excited singlet state. The porphyrin dyad **11** was excited at 300 nm, and emission was monitored at 650 nm. A single exponential decay was observed, with a time constant of 10.0 ns (χ^2 = 1.20). This lifetime is typical of free base tetraarylporphyrins, and shows that the slight excitonic interaction of the Soret bands does not affect the lifetime of the porphyrin first excited singlet state.

The tetrads **13** and **14** and hexad **1** were all investigated in a similar manner with excitation at 300 nm, where most of the absorption is due to the coumarins. When the coumarin emission was monitored at 490 nm, all three compounds gave exponential decays with lifetimes of <10 ps. These lifetimes were too short to measure accurately using the apparatus employed but are drastically shorter than the ca. 2.5 ns lifetimes observed for the coumarin model compounds, and are consistent with quenching of the coumarin excited states by singlet energy transfer to the porphyrin moieties. When the emission was monitored at 650 nm, where only porphyrin fluoresces, lifetimes of 10 ns were observed for all three compounds. Thus, the porphyrin excited singlet states are not quenched at all by the coumarin moieties.

Transient Absorption Experiments. The fluorescence results showed that quenching of the coumarin excited states by the porphyrin moieties was too fast to resolve using the single photon timing apparatus. Thus, we turned to pump−probe transient absorption experiments with sub-picosecond laser excitation to learn more about the quenching process. Excitation of a 2-methyltetrahydrofuran solution of hexad **1** with 450 nm, ~100 fs laser pulses yielded the transient spectra shown in Figure 7. At times less than a few ps, the spectra show

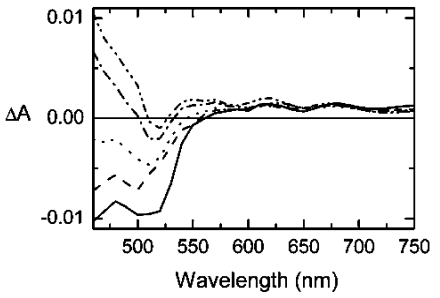

Figure 7. Transient absorption spectra for hexad **1** in 2-methyltetrahydrofuran following excitation at 450 nm. Spectra are shown at 0 ps (solid), 0.5 ps (dash), 1 ps (dot), 4 ps (dash-dot), and 15 ps (dash-dot-dot) after the excitation flash.

mainly stimulated emission from the coumarins in the <550 nm region. At later times, the absorbance change is mostly positive, and has the characteristic features of the porphyrin excited state, which is being formed as the coumarin excited states decay. These features are all consistent with energy transfer from the coumarins to the porphyrin moieties.

Kinetic studies were carried out both on **1** and on the model compounds with measurement at 480 nm, where the coumarin stimulated emission is decaying and the porphyrin transient absorption is growing in concurrently (see Figure 7). Results are shown in Figure 8. For dyad **12**, which features a single coumarin in an *ortho* relationship to a single porphyrin, the kinetics were fitted with three exponential processes. Two of these had time constants of 0.8 ps (85%) and 3.4 ps (15%), and the third did not decay appreciably on this time scale. With tetrad **13**, wherein both porphyrin moieties are *ortho* to a coumarin chromophore, three processes were also observed. Two had time constants of 0.9 ps (75%) and 3.8 ps (25%), and the third transient decayed only very slowly on this time scale.

dx.doi.org/10.1021/jp402265e | J. Phys. Chem. B XXXX, XXX, XXX−XXX

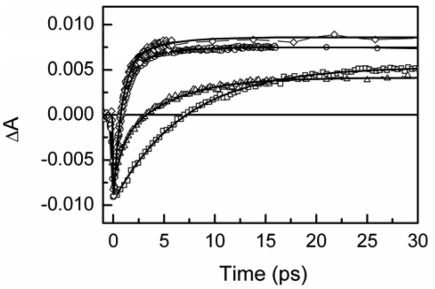

Figure 8. Normalized transient kinetics at 480 nm for dyad **12** (diamonds), tetrad **13** (circles), tetrad **14** (squares), and hexad **1** (triangles). Fitting gave the time constants reported in the text.

The similar results for these two molecules suggest that, in both cases, the coumarin excited singlet states are decaying mainly by singlet−singlet energy transfer to the porphyrin *ortho* to it. Fluorescence upconversion measurements confirm that the two short components are indeed due to coumarin fluorescence decay (Supporting Information). The two short kinetic components suggest that there are two populations of molecules, a major (75%) and a minor (25%) population, that differ in the separation and orientation of the porphyrin and coumarin moieties, and therefore show different energy transfer rates. This is reasonable, given the various rotational possibilities around the single bonds in the ester linkage joining the coumarins to the hexaphenylbenzene. For each population of **13**, the energy transfer rate constant k_{ent} is given by eq 1, where τ_m is the measured decay time

$$k_{ent} = \frac{1}{\tau_m} - \frac{1}{\tau_0} \quad (1)$$

constant and τ_0 is the lifetime of the coumarin first excited singlet state in the absence of energy transfer. The value of τ_0 is taken as 2.4 ns from the fluorescence studies of **10** mentioned above. This yields $k_{ent} = 1.1 \times 10^{12}$ s^{-1} for the major conformer and $k_{ent} = 2.6 \times 10^{11}$ s^{-1} for the minor conformer. It is possible that there are actually more than two populated conformers giving more than two rate constants, but the kinetic traces were fitted satisfactorily by two short components, within the limits imposed by the signal-to-noise ratio obtained in our measurements. The third transient observed for **12** and **13**, which did not decay appreciably on the time scale of our measurement, is assigned to the decay of the porphyrin first excited singlet state, which has a time constant of 10 ns, based on the fluorescence lifetime results mentioned above.

Turning now to tetrad **14**, in which the coumarin moieties are *meta* to the nearest porphyrin, the kinetic results were fitted as three exponential components with time constants of 3.4 ps (20%), 7.5 ps (80%), and a component that decayed too slowly to measure on this time scale. As with **12** and **13**, the long component is assigned to decay of the porphyrin first excited singlet state, and the two shorter components to decay of the coumarin excited states by energy transfer to the porphyrins. These assignments are confirmed by fluorescence upconversion results (Supporting Information). Again, two conformers are postulated: a minor (20%) component with $\tau_m = 3.4$ ps and a major (80%) component with $\tau_m = 7.5$ ps. From eq 1, the energy transfer rate constant for the minor component is $k_{ent} = 2.9 \times 10^{11}$ s^{-1} and that for the major component is $k_{ent} = 1.3 \times 10^{11}$ s^{-1}.

The kinetic trace for hexad **1** was fitted with three components of 1.0 ps (45%), 5.5 ps (55%), and a component that did not decay appreciably on the time scale of measurement. Although the coumarins in **1** will not be able to sample exactly the same conformations that they can in **13** and **14**, we can still use the results for these models to gain insight into the interpretation of the results for **1**. The nondecaying component is assigned to the porphyrin first excited singlet state, which has a lifetime of 10 ns. The other two components are due to energy transfer from the four coumarin moieties to the two porphyrins. By comparison with the results for **12** and **13**, we note that the 1.0 ps component is similar to the time constant for energy transfer from the major conformation of the coumarin moieties *ortho* to porphyrins in **12** and **13** to generate the porphyrin first excited singlet state (0.9 ps). Thus, this component must be due mainly to a similar process in **1**. The 5.5 ps component must be associated with energy transfer involving any minor conformation(s) of the *ortho* coumarins and both major and minor conformations of the coumarins *meta* to the nearest porphyrin. The 5.5 ps decay is longer than either the long energy transfer decay component of **13** (3.8 ps) or the short energy transfer component of **14** (3.4 ps). It likely includes some contribution from energy transfer from an analogue of the major conformer of **14**. Our data does not permit us to resolve three or more components on the 1−10 ps time scale for **1**, and the 5.5 ps decay may represent a mixture of processes with similar time constants.

It is not possible to adequately simulate the actual decay data for **1** using the four time constants measured for models **13** and **14** in the amplitude ratios observed in those compounds. It seems likely that, in **1**, the conformations available to the coumarin moieties and their population ratios will differ from those observed in the model compounds due to steric repulsions and perhaps attractive interactions among the coumarin moieties. It is also likely that singlet energy is transferred between adjacent coumarins. Indeed, anisotropy studies of **9** and **10** suggest that inter-coumarin energy transfer on the time scale of about 7 ps also contributes to the overall transfer of excitation energy from the coumarins to the porphyrins (see the Supporting Information).

The quantum yield of singlet−singlet energy transfer from any of the excited coumarin antenna molecules to a porphyrin is 1.0, which is consistent with the less accurate value of 93% derived from the fluorescence excitation spectra. In terms of quantum efficiency, the coumarin system is a near-perfect antenna for the porphyrins.

Heptad 2 and Photoinduced Electron Transfer. Hexad **1** efficiently delivers the excitation resulting from absorption by any of the chromophores to the porphyrin moieties but is only an antenna system, as there is no provision for reaction center function. The fact that the lifetimes of the first excited singlet states of the porphyrins of **1** are essentially the same as those of model porphyrins and **11** shows that the porphyrin does not decay by photoinduced electron transfer. However, reaction center function can be added. Introduction of a zinc atom into each of the porphyrins of **1** gives **1Zn**, in which the zinc atoms are capable of coordination of a fifth ligand. As we have shown with similar molecules,[36,47] fullerene **7** coordinates to the two zinc atoms of **1Zn** to yield heptad **2**. By analogy with the compounds studied earlier, the coordinated fullerene is expected to accept an electron from an excited zinc porphyrin to yield a charge-separated state.

dx.doi.org/10.1021/jp402265e | J. Phys. Chem. B XXXX, XXX, XXX−XXX

Hexad **1Zn** was prepared by a synthetic route closely related to that employed for **1** (see the Supporting Information). Addition of an excess of dipyridylfullerene **7** resulted in complex formation to yield **2**. Good binding was observed in 1,2-difluorobenzene, where the binding constant measured in a very similar system was 7.3×10^4 M^{-1}.[47] The absorption spectra of **2** and some model compounds in this solvent are shown in Figure 9. The spectrum of **1Zn** features a Soret

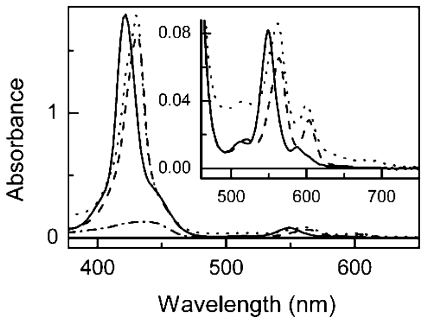

Figure 9. Absorption spectra in 1,2-difluorobenzene of heptad **2** (dotted), **1Zn** (solid), **1Zn** plus excess dipyridyl alcohol **15** (dash), and coumarin model **9** (dash-dot). The alcohol **15** and the fullerene **7** used to form complex **2** were added to the 1,2-difluorobenzene solution after they were dissolved in a minimum amount of CS_2, for reasons of solubility.

maximum at 421 nm, a shoulder due to the coumarin moieties at ca. 445 nm, and zinc porphyrin Q-band absorption at 512, 549, and 588 nm. When excess dipyridyl alcohol **15** dissolved in a minimum amount of CS_2 was added to the solution, complex formation with **1Zn** was observed. This resulted in a shift of the porphyrin bands to longer wavelengths, so that the Soret appeared at 431 nm and the Q-band absorptions shifted to 520, 564, and 603 nm. Addition of fullerene **7** to **1Zn** led to complex formation to form **2**, and to similar shifts in the absorption spectrum. The fullerene was dissolved in a minimum amount of CS_2 and the resulting solution was added to the hexad **1Zn** in 1,2-difluorobenzene. The Soret of **2** was found at 431, and Q-band maxima at 518, 562, and 600 nm. The fullerene ligand absorbs weakly throughout the visible down to 690 nm, where a small maximum appears. The absorption of coumarin model compound **9** is also shown in Figure 9. The maximum absorption is at 438 nm, which represents a shift of about 6 nm to longer wavelengths on going from 2-methyltetrahydrofuran to 1,2-difluorobenzene.

The fluorescence spectra of these compounds in 1,2-difluorobenzene were also measured. A solution of **1Zn** showed emission maxima at 592 and 649 nm, which is typical of zinc tetraarylporphyrins of this type. When dipyridyl alcohol **15** was added, the maxima appeared at 615 and 667 nm. Thus, there is a significant shift to longer wavelengths upon addition of the ligand. Heptad **2** shows no detectable steady-state emission, which is consistent with quenching of the zinc porphyrin excited state by photoinduced electron transfer to the fullerene. Coumarin model **9** shows emission at 472 nm in 1,2-difluorobenzene, which is a 7 nm shift to longer wavelengths relative to 2-methyltetrahydrofuran.

Transient absorption studies were also carried out on these materials in 1,2-difluorobenzene with ~100 fs excitation pulses at 450 nm (Figure 10). For **1Zn**, the decay at 490 nm could be fitted by exponentially increasing components of 1.1 ps (50%) and 6.7 ps (50%), and exponentially decreasing components of

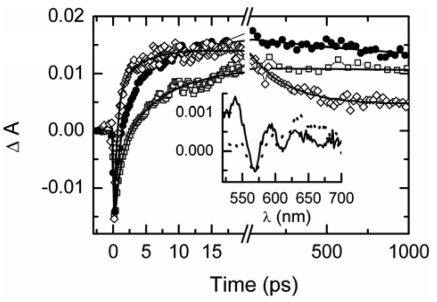

Figure 10. Transient absorption kinetics at 490 nm in 1,2-difluorobenzene with excitation at 450 nm for **1Zn** (squares), **1Zn** after addition of excess dipyridyl alcohol **15** (circles), and **1Zn** after addition of excess fullerene **7** to form **2** (diamonds). Note the break in the time axis. The solid lines through the symbols show the results of fitting as discussed in the text. The inset shows spectra 30 ps after excitation for **1Zn** plus **15** (solid line) and **2** (dotted line).

2.2 ns and a component that does not decay appreciably on this time scale. As with **1**, the two short components are due to the decay of the coumarin first excited singlet states and concurrent formation of the porphyrin first excited singlet states via singlet−singlet energy transfer. The third component is due to the porphyrin first excited singlet state. Its lifetime could not be determined precisely on this time scale. However, time-resolved fluorescence experiments on the zinc form of dyad **11**, **11Zn**, with excitation at 420 nm and emission at 620 nm yielded a time constant of 2.2 ns for this decay ($\chi^2 = 1.19$). It is assumed that the lifetime of the porphyrin excited singlet state of **1Zn** is similar, and this lifetime gives a satisfactory fit to the data (Figure 10). The final, nondecaying component is ascribed to the porphyrin triplet state.

When dipyridyl alcohol **15** was added to the solution of **1Zn**, a complex formed, and fitting of the transient absorbance at 490 nm yielded rising components of 0.9 ps (50%) and 5.8 ps (50%), an exponential decay of 1.6 ns, and a component that does not decay on this time scale. Transient fluorescence studies on a solution of **11Zn** containing an excess of **15** yielded an exponential decay at 620 nm with a time constant of 1.57 ns ($\chi^2 = 1.16$), and based on this model, the 1.6 ns decay component of **1Zn** with the pyridyl alcohol present is ascribed to a porphyrin excited singlet state with a similar lifetime. The nondecaying component is again ascribed to the porphyrin triplet state. Thus, singlet energy transfer from the coumarin moieties of **1Zn** to the zinc porphyrins is very slightly faster when the pyridine ligand is present, and the lifetime of the porphyrin excited singlet state is slightly shorter.

Fullerene **7** was added to the solution of **1Zn** in 1,2-difluorobenzene to yield **2**, and the resulting solution studied by transient absorption (Figure 10). With excitation at 450 nm, kinetics at 490 nm were found to include two short, rising components with time constants of 0.6 ps (80%) and 4.3 ps (20%), plus a decay component with a time constant of 230 ps. The 230 ps decay is associated with the decay of a $P^{\bullet+}-C_{60}^{\bullet-}$ charge-separated state formed by photoinduced electron transfer from the porphyrin excited singlet state to the fullerene. This time constant is similar to those observed for decay of the charge-separated state in similar molecules lacking the coumarin antennas.[36,47] The spectral signature of the porphyrin radical cation is apparent in the 650 nm region, as seen in the inset spectrum in Figure 10. The time constant for formation of the charge-separated state was not separately resolved in these studies. Studies of similar molecules without

dx.doi.org/10.1021/jp402265e | J. Phys. Chem. B XXXX, XXX, XXX−XXX

the coumarin antennas in the same solvent give a time constant for photoinduced electron transfer of 3 ps.[36,47] In the case of **2**, the electron transfer time constant is thus on the order of those for singlet energy transfer from the coumarin antennas, and the measured 0.6 and 4.3 ps time constants actually represent two or more energy transfer processes and one electron transfer process, all of which occur with roughly comparable time constants.

DISCUSSION

The energy and electron transfer properties of **1** and **2** may be discussed with reference to Figure 11, which shows the various

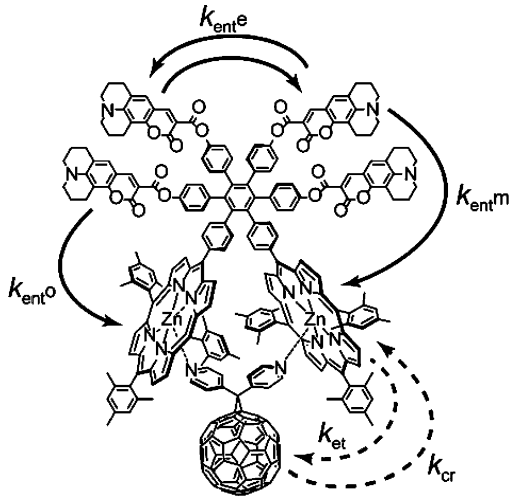

Figure 11. Pathways for singlet−singlet energy transfer (k_{ent}), photoinduced electron transfer (k_{et}), and charge recombination (k_{cr}) in heptad **2**. Similar pathways are present in hexad **1**, except that electron transfer does not occur. Rate constants are given in the text.

energy and electron transfer pathways. Rate constants for these processes may be deduced from the results for the various model compounds and for **1** and **2** themselves. On the basis of the results for **1** and models **13** and **14**, excitation of a coumarin *ortho* to a porphyrin of hexad **1** in 2-methyltetrahydrofuran is followed by singlet−singlet energy transfer to that porphyrin with rate constants ($k_{ent,o}$) of 1.1×10^{12} s^{-1}. Minor conformations of the *ortho* coumarins may also be present, with transfer rate constants of about 3×10^{11} s^{-1}. A coumarin *meta* to a porphyrin also shows energy transfer directly to that porphyrin with rate constants $k_{ent,m}$ of about 1×10^{11} to 3×10^{11} s^{-1}. Transfer from a *meta* coumarin to a porphyrin may also occur by a stepwise migration of energy from a *meta* coumarin to an *ortho* coumarin, and then on to the porphyrin. The largest rate constants for inter-coumarin energy transfer are ca. 1×10^{11} s^{-1}. Energy transfer from a coumarin moiety to a porphyrin *para* to it is too slow to compete with the energy transfer processes discussed above. Overall, light absorbed by any of the coumarin moieties is transferred to a porphyrin with a quantum yield of essentially unity. Thus, the coumarins are highly efficient antennas for porphyrins in the spectral region where they absorb strongly. Coumarin absorption contributes a relatively small amount to the overall absorption cross section of **1** in the Soret region because the porphyrin Soret extinction coefficient is exceedingly large. However, the coumarin light collection properties in the 430−460 region are significant because the porphyrin absorbs very little at these wavelengths.

Self-assembly of hexad **1Zn** with fullerene **7** produced antenna−reaction center complex **2**. For **2** in 1,2-difluorobenzene, $k_{ent,o}$ and $k_{ent,m}$ for all conformations are $\geq 1.8 \times 10^{11}$ s^{-1}, and energy transfer from coumarin to zinc porphyrin has a quantum yield of 1.0. Exchange of excitation energy between the coumarins ($k_{ent,e}$) on the same time scale also likely contributes. The zinc porphyrin excited singlet state decays by photoinduced electron transfer ($k_{et} = 3.3 \times 10^{11}$ s^{-1}, Figure 11) to give the $P^{\bullet+}-C_{60}^{\bullet-}$ charge separated state with an overall quantum yield of unity based on light absorbed by the coumarin antennas or directly by the porphyrins. The charge-separated state decays with a time constant of 230 ps ($k_{cr} = 4.4 \times 10^{9}$ s^{-1}).

Singlet−singlet energy transfer in systems such as these may be explained in principle by the simple Förster dipole−dipole mechanism, but Dexter-type electron exchange energy transfer may also play a role. Rotation is possible about the three single bonds in the linkages joining the coumarin moieties to the hexaphenylbenzene ring, and it is likely that two or more conformations are populated. Indeed, the two energy transfer rate constants for energy transfer measured for **13**, **14**, and **1** are likely averages of rate constants for several conformations that gave satisfactory fits to the kinetic data. Molecular mechanics modeling (MM2) yields possible distances between the center of an *ortho* coumarin and the center of the nearest porphyrin of 8−14 Å. Calculations using simple Förster theory, a distance of 11 Å, and a random orientation factor (κ^2) of 2/3 yield $k_{ent,o} = 7 \times 10^{11}$ s^{-1}, which is close to the rate constant observed for the major conformer of **13**. For a *meta* coumarin, the molecular mechanics calculations yield a range of distances of 14−21 Å for the separation of the coumarin and the *meta* porphyrin. The Förster calculations based on a separation of 14 Å yield $k_{ent,m} = 1.7 \times 10^{11}$ s^{-1}, which is similar to the measured values for **14**. Thus, singlet−singlet energy transfer in **1** is consistent with expectations from simple Förster dipole−dipole theory, and invoking exchange energy transfer is not necessary. This is in contrast to the situation in another hexaphenylbenzene-based system, where bis(phenylethynyl)anthracene (BPEA) antennas were employed.[34] In that case, there was evidence for exchange-mediated singlet−singlet energy transfer from BPEA to porphyrin. However, the linkages joining the BPEA moieties to the central benzene ring could at least formally provide some conjugative interactions with the porphyrin, whereas, in the case of the coumarin antennas, the single bonds in the ester linkages are not expected to mediate exchange coupling as well.

Photoinduced electron transfer in heptad **2** was found to occur very rapidly and efficiently, with a time constant consistent with that measured for another molecule with essentially the same diporphyrin−fullerene dative linkage but no antenna moieties.[48] The lifetime of the charge-separated state, 230 ps, was also the same as that reported for the molecule studied earlier. Although the $P^{\bullet+}-C_{60}^{\bullet-}$ charge separated state formed in **2** was produced with a quantum yield of unity, the lifetime is shorter than would be ideal for some applications in solar energy conversion, sensing, etc. As has been shown previously, longer lifetimes may be achieved by employing linkages with less electronic coupling between the donor and acceptor, and the use of multistep electron transfer schemes.[10,11]

dx.doi.org/10.1021/jp402265e | J. Phys. Chem. B XXXX, XXX, XXX−XXX

CONCLUSIONS

These studies show that coumarin moieties are well suited as antennas in the 400−460 nm spectral range for porphyrin-based artificial photosynthetic reaction centers. For the systems studied here, efficiencies of singlet−singlet energy transfer from coumarins to nearby porphyrins were essentially unity in spite of the relatively long, flexible ester linkages between the coumarins and the hexaphenylbenzene ring. The high transfer rates and therefore efficiencies are ensured by coumarin singlet excited state lifetimes of several ns and high fluorescence quantum yields—qualities not shared by natural carotenoid antennas that absorb in similar spectral regions. Because of the very rapid nonradiative decay processes and infinitesimal fluorescence quantum yields of carotenoids, efficient antenna function requires stringent control over interchromophore separations and orientations.[49−55] As a result, in natural photosynthesis, very subtle changes in the protein environment can be used to implement large changes in the yields of energy and electron transfer processes which in turn lead to mechanisms for photoprotection and control of excitation energy.

In this and related research, we have identified several classes of chromophores, including coumarins, bis(phenylethynyl)-anthracenes,[34−36] boron dipyrromethenes,[36] and synthetic carotenoids,[49−55] that can act as antennas for porphyrin-based artificial reaction centers, and in concert can harvest light efficiently across the entire visible spectral region. Achieving high efficiency in a synthetic system for producing fuel or electricity using sunlight requires efficient light absorption from around 400 nm to the 1000 nm region. The highest efficiencies require tandem photoconversion systems with two or more photoactive components that cover this spectral region.[56] It seems likely that practical photoconversion systems may require antenna moieties of various types in order to drive conversion of light to useful forms of energy via artificial photosynthesis. The use of antennas such as those described here can also be combined with photoprotective and photoregulatory functions in artificial photosynthesis, as inspired by similar processes in biology.[57,58]

ASSOCIATED CONTENT

Supporting Information

Experimental details of the synthesis and characterization, fluorescence upconversion data, and anisotropy data. This material is available free of charge via the Internet at http://pubs.acs.org.

AUTHOR INFORMATION

Corresponding Author

*E-mail: gust@asu.edu (D.G.); tmoore@asu.edu (T.A.M.); amoore@asu.edu (A.L.M.).

Notes

The authors declare no competing financial interest.

ACKNOWLEDGMENTS

Research supported by the U.S. Department of Energy, Office of Basic Energy Sciences, under Award No. DE-FG02-03ER15393 (synthetic and photoelectrochemical studies) and as part of the Center for Bio-Inspired Solar Fuel Production, an Energy Frontier Research Center funded by the U.S. Department of Energy, Office of Science, Office of Basic Energy Sciences, under Award No. DE-SC0001016 (spectroscopic and transient spectroscopic studies).

REFERENCES

(1) Demmig-Adams, B.; Adams, W. W., III. Antioxidants in Photosynthesis and Human Nutrition. *Science* **2002**, *298*, 2149−2153.
(2) Ahn, T. K.; Avenson, T. J.; Ballottari, M.; Cheng, Y. C.; Niyogi, K. K.; Bassi, R.; Fleming, G. R. Architecture of a Charge-Transfer State Regulating Light Harvesting in a Plant Antenna Protein. *Science* **2008**, *320*, 794−797.
(3) Berera, R.; van Stokkum, I. H. M.; d'Haene, S.; Kennis, J. T. M.; van Grondelle, R.; Dekker, J. P. A Mechanism of Energy Dissipation in Cyanobacteria. *Biophys. J.* **2009**, *96*, 2261−2267.
(4) Ruban, A. V.; Berera, R.; Ilioaia, C.; van Stokkum, I. H. M.; Kennis, J. T. M.; Pascal, A. A.; van Amerongen, H.; Robert, B.; Horton, P.; van Grondelle, R. Identification of a Mechanism of Photoprotective Energy Dissipation in Higher Plants. *Nature* **2007**, *450*, 575−578.
(5) Li, X. P.; Gilmore, A. M.; Caffarri, S.; Bassi, R.; Golan, T.; Kramer, D.; Niyogi, K. K. Regulation of Photosynthetic Light Harvesting Involves Intrathylakoid Lumen pH Sensing by the PsbS Protein. *J. Biol. Chem.* **2004**, *279*, 22866−22874.
(6) Cogdell, R. J.; Frank, H. A. How Carotenoids Function in Photosynthetic Bacteria. *Biochim. Biophys. Acta* **1987**, *895*, 63−79.
(7) Mathis, P.; Schenck, C. C. In *Carotenoid Chemistry and Biochemistry*; Britton, G., Goodwin, T. W., Eds.; Pergamon: Oxford, U.K., 1981.
(8) Polivka, T.; Sundstrom, V. Ultrafast Dynamics of Carotenoid Excited States - From Solution to Natural and Artificial Systems. *Chem. Rev.* **2004**, *104*, 2021−2071.
(9) Sauer, K. Photosynthetic Membranes. *Acc. Chem. Res.* **1978**, *11*, 257−264.
(10) Gust, D.; Moore, T. A.; Moore, A. L. Solar Fuels via Artificial Photosynthesis. *Acc. Chem. Res.* **2009**, *42*, 1890−1898.
(11) Gust, D.; Moore, T. A.; Moore, A. L. Realizing Artificial Photosynthesis. *Faraday Discuss.* **2012**, *155*, 9−26.
(12) Meyer, T. J. Chemical Approaches to Artificial Photosynthesis. *Acc. Chem. Res.* **1989**, *22*, 163−170.
(13) Wasielewski, M. R. Photoinduced Electron Transfer in Supramolecular Systems for Artificial Photosynthesis. *Chem. Rev.* **1992**, *92*, 435−461.
(14) Garg, V.; Kodis, G.; Chachisvilis, M.; Hambourger, M.; Moore, A. L.; Moore, T. A.; Gust, D. Conformationally Constrained Macrocyclic Diporphyrin-Fullerene Artificial Photosynthetic Reaction Center. *J. Am. Chem. Soc.* **2011**, *133*, 2944−2954.
(15) Kodis, G.; Liddell, P. A.; de la Garza, L.; Clausen, P. C.; Lindsey, J. S.; Moore, A. L.; Moore, T. A.; Gust, D. Efficient Energy Transfer and Electron Transfer in an Artificial Photosynthetic Antenna-Reaction Center Complex. *J. Phys. Chem. A* **2002**, *106*, 2036−2048.
(16) Kuciauskas, D.; Liddell, P. A.; Lin, S.; Johnson, T. E.; Weghorn, S. J.; Lindsey, J. S.; Moore, A. L.; Moore, T. A.; Gust, D. An Artificial Photosynthetic Antenna-Reaction Center Complex. *J. Am. Chem. Soc.* **1999**, *121*, 8604−8614.
(17) Aratani, N.; Osuka, A.; Kim, Y. H.; Jeong, D. H.; Kim, D. Extremely Long, Discrete Meso-Meso-Coupled Porphyrin Arrays. *Angew. Chem., Int. Ed. Engl.* **2000**, *39*, 1458−1462.
(18) Bothner-By, A. A.; Dadok, J.; Johnson, T. E.; Lindsey, J. S. Molecular Dynamics of Covalently-Linked Multi-Porphyrin Arrays. *J. Phys. Chem.* **1996**, *100*, 17,551−17,557.
(19) Burrell, A. K.; Officer, D. L.; Plieger, P. G.; Reid, D. C. W. Synthetic Routes to Multiporphyrin Arrays. *Chem. Rev.* **2001**, *101*, 2751−2796.
(20) Guldi, D. M. Fullerene-Porphyrin Architectures; Photosynthetic Antenna and Reaction Center Models. *Chem. Soc. Rev.* **2002**, *31*, 22−36.
(21) Harriman, A. Energy Transfer in Synthetic Porphyrin Arrays. In *Supramolecular Photochemistry*; Balzani, V., Ed.; D. Reidel Publishing Company: Dordrecht, Holland, 1987; pp 207−223.
(22) Li, J.; Ambroise, A.; Yang, S. I.; Diers, J. R.; Seth, J.; Wack, C. R.; Bocian, D. F.; Holten, D.; Lindsey, J. S. Template-Directed Synthesis,

Excited State Photodynamics, and Electronic Communication in a Hexameric Wheel of Porphyrins. *J. Am. Chem. Soc.* **1999**, *121*, 8927−8940.
(23) Li, J.; Diers, J. R.; Seth, J.; Yang, S. I.; Bocian, D. F.; Holten, D.; Lindsey, J. S. Synthesis and Properties of Star-Shaped Multiporphyrin-Phthalocyanine Light-Harvesting Arrays. *J. Org. Chem.* **1999**, *64*, 9090−9100.
(24) Lin, V. S. Y.; Dimagno, S. G.; Therien, M. J. Highly Conjugated, Acetylenyl Bridged Porphyrins: New Models for Light-Harvesting Antenna Systems. *Science* **1994**, *264*, 1105−1111.
(25) Nakano, A.; Osuka, A.; Yamazaki, I.; Yamazaki, T.; Nishimura, Y. Windmill-Like Porphyrin Arrays as Potent Light-Harvesting Antenna Complexes. *Angew. Chem., Int. Ed. Engl.* **1998**, *37*, 3023−3027.
(26) Paolesse, R.; Jaquinod, L.; Della Sala, F.; Nurco, D. J.; Prodi, L.; Montalti, M.; Di Natale, C.; D'Amico, A.; Di Carlo, A.; Lugli, P.; et al. Beta-Fused Oligoporphyrins: A Novel Approach to a New Type of Extended Aromatic System. *J. Am. Chem. Soc.* **2000**, *122*, 11295−11302.
(27) Rucareanu, S.; Mongin, O.; Schuwey, A.; Hoyler, N.; Gossauer, A.; Amrein, W.; Hediger, H.-U. Supramolecular Assemblies Between Macrocyclic Porphyrin Hexamers and Star-Shaped Porphyrin Arrays. *J. Org. Chem.* **2001**, *66*, 4973−4988.
(28) Cho, H. S.; Rhee, H.; Song, J. K.; Min, C.-K.; Takase, M.; Aratani, N.; Cho, S.; Osuka, A.; Joo, T.; Kim, D. Excitation Energy Transport Processes of Porphyrin Monomer, Dimer, Cyclic Trimer, and Hexamer Probed by Ultrafast Fluorescence Anisotropy Decay. *J. Am. Chem. Soc.* **2003**, *125*, 5849−5860.
(29) Brodard, P.; Matzinger, S.; Vauthey, E.; Mongin, O.; Papamicaël, C.; Gossauer, A. Investigations of Electronic Energy Transfer Dynamics in Multiporphyrin Arrays. *J. Phys. Chem. A* **1999**, *103*, 5858−5870.
(30) Hwang, I.-W.; Kamada, T.; Ahn, T. K.; Ko, D. M.; Nakamura, T.; Tsuda, A.; Osuka, A.; Kim, D. Porphyrin Boxes Constructed by Homochiral Self-Sorting Assembly: Optical Separation, Exciton Coupling, and Efficient Excitation Energy Migration. *J. Am. Chem. Soc.* **2004**, *126*, 16187−16198.
(31) Morandeira, A.; Vauthey, E.; Schuwey, A.; Gossauer, A. Ultrafast Excited State Dynamics of Tri- and Hexaporphyrin Arrays. *J. Phys. Chem. A* **2004**, *108*, 5741−5751.
(32) Nakamura, Y.; Hwang, I.-W.; Aratani, N.; Ahn, T. K.; Ko, D. M.; Takagi, A.; Kawai, T.; Matsumoto, T.; Kim, D.; Osuka, A. Directly Meso-Meso Linked Porphyrin Rings: Synthesis, Characterization, and Efficient Excitation Energy Hopping. *J. Am. Chem. Soc.* **2005**, *127*, 236−246.
(33) Aratani, N.; Osuka, A.; Cho, H. S.; Kim, D. Photochemistry of Covalently-Linked Multiporphyrinic Systems. *J. Photochem. Photobiol., C* **2002**, *3*, 25−52.
(34) Kodis, G.; Terazono, Y.; Liddell, P. A.; Andréasson, J.; Garg, V.; Hambourger, M.; Moore, T. A.; Moore, A. L.; Gust, D. Energy and Photoinduced Electron Transfer in a Wheel-Shaped Artificial Photosynthetic Antenna-Reaction Center Complex. *J. Am. Chem. Soc.* **2006**, *128*, 1818−1827.
(35) Terazono, Y.; Liddell, P. A.; Garg, V.; Kodis, G.; Brune, A.; Hambourger, M.; Moore, T. A.; Moore, A. L.; Gust, D. Artificial Photosynthetic Antenna-Reaction Center Complexes Based on a Hexaphenylbenzene Core. *J. Porphyrins Phthalocyanines* **2005**, *9*, 706−723.
(36) Terazono, Y.; Kodis, G.; Liddell, P. A.; Garg, V.; Moore, T. A.; Moore, A. L.; Gust, D. Multiantenna Artificial Photosynthetic Reaction Center Complex. *J. Phys. Chem. B* **2009**, *113*, 7147−7155.
(37) Springer, J. W.; Parkes-Loach, P. S.; Reddy, K. R.; Krayer, M.; Jiao, J.; Lee, G. M.; Niedzwiedzki, D. M.; Harris, M. A.; Kirmaier, C.; Bocian, D. F.; et al. Biohybrid Photosynthetic Antenna Complexes for Enhanced Light-Harvesting. *J. Am. Chem. Soc.* **2012**, *134*, 4589−4599.
(38) Iehl, J.; Nierengarten, J. F.; Harriman, A.; Bura, T.; Ziessel, R. Artificial Light-Harvesting Arrays: Electronic Energy Migration and Trapping on a Sphere and Between Spheres. *J. Am. Chem. Soc.* **2012**, *134*, 988−998.
(39) Dutta, P. K.; Varghese, R.; Nangreave, J.; Lin, S.; Yan, H.; Liu, Y. DNA-Directed Artificial Light-Harvesting Antenna. *J. Am. Chem. Soc.* **2011**, *133*, 11985−11993.
(40) Adeyemi, O. O.; Malinovskii, V. L.; Biner, S. M.; Calzaferri, G.; Haener, R. Photon Harvesting by Excimer-Forming Multichromophores. *Chem. Commun.* **2012**, *48*, 9589−9591.
(41) Oltra, N. S.; Browne, W. R.; Roelfes, G. Hierarchical Self-Assembly of a Biomimetic Light-Harvesting Antenna Based on DNA G-Quadruplexes. *Chem.—Eur. J.* **2013**, *19*, 2457−2461.
(42) Ghiggino, K. P.; Bell, T. D.; Hooley, E. N. Synthetic Polymers for Solar Harvesting. *Faraday Discuss.* **2012**, *155*, 79−88.
(43) Loiseau, F.; Marzanni, G.; Quici, S.; Indelli, M. T.; Campagna, S. An Artificial Antenna Complex Containing Four Ru(Bpy)(3)(2+)-Type Chromophores as Light-Harvesting Components and a Ru(Bpy)(CN)(4)(2-) Subunit as the Energy Trap. A Structural Motif Which Resembles the Natural Photosynthetic Systems. *Chem. Commun.* **2003**, 286−287.
(44) Jung, H.; Gulis, G.; Gupta, S.; Redding, K.; Gosztola, D. J.; Wiederrecht, G. P.; Stroscio, M. A.; Dutta, M. Optical and Electrical Measurement of Energy Transfer Between Nanocrystalline Quantum Dots and Photosystem I. *J. Phys. Chem. B* **2010**, *114*, 14544−14549.
(45) Nabiev, I.; Rakovich, A.; Sukhanova, A.; Lukashev, E.; Zagidullin, V.; Pachenko, V.; Rakovich, Y. P.; Donegan, J. F.; Rubin, A. B.; Govorov, A. O. Fluorescent Quantum Dots As Artificial Antennas for Enhanced Light Harvesting and Energy Transfer to Photosynthetic Reaction Centers. *Angew. Chem., Int. Ed.* **2010**, *49*, 7217−7221.
(46) Lindsey, J. S.; Prathapan, S.; Johnson, T. E.; Wagner, R. W. Porphyrin Building Blocks for Modular Construction of Bioorganic Model Systems. *Tetrahedron* **1994**, *50*, 8941−8968.
(47) Terazono, Y.; Kodis, G.; Liddell, P. A.; Garg, V.; Gervaldo, M.; Moore, T. A.; Moore, A. L.; Gust, D. Photoinduced Electron Transfer in a Hexaphenylbenzene-Based Self-Assembled Porphyrin-Fullerene Triad. *Photochem. Photobiol.* **2007**, *83*, 464−469.
(48) Ramachandran, G. K.; Tomfohr, J. K.; Li, J.; Sankey, O. F.; Zarate, X.; Primak, A.; Terazono, Y.; Moore, T. A.; Moore, A. L.; Gust, D.; et al. Electron Transport Properties of a Carotene Molecule in a Metal-(Single Molecule)-Metal Junction. *J. Phys. Chem. B* **2003**, *107*, 6162−6169.
(49) Berera, R.; van Stokkum, I. H. M.; Kodis, G.; Keirstead, A. E.; Pillai, S.; Herrero, C.; Palacios, R. E.; Vengris, M.; van Grondelle, R.; Gust, D.; et al. Energy Transfer, Excited-State Deactivation, and Exciplex Formation in Artificial Caroteno-Phthalocyanine Light-Harvesting Antennas. *J. Phys. Chem. B* **2007**, *111*, 6868−6877.
(50) Kloz, M.; Pillai, S.; Kodis, G.; Gust, D.; Moore, T. A.; Moore, A. L.; van Grondelle, R.; Kennis, J. T. M. New Light-Harvesting Roles of Hot and Forbidden Carotenoid States in Artificial Photosynthetic Constructs. *Chem. Sci.* **2012**, *3*, 2052−2061.
(51) Kodis, G.; Herrero, C.; Palacios, R.; Mariño-Ochoa, E.; Gould, S. L.; de la Garza, L.; van Grondelle, R.; Gust, D.; Moore, T. A.; Moore, A. L.; et al. Light Harvesting and Photoprotective Functions of Carotenoids in Compact Artificial Photosynthetic Antenna Designs. *J. Phys. Chem. B* **2004**, *108*, 414−425.
(52) Bensasson, R. V.; Land, E. J.; Moore, A. L.; Crouch, R. L.; Dirks, G.; Moore, T. A.; Gust, D. Mimicry of Antenna and Photoprotective Carotenoid Functions by a Synthetic Carotenoporphyrin. *Nature* **1981**, *290*, 329−332.
(53) Gust, D.; Moore, T. A. Mimicking Photosynthesis. *Science* **1989**, *244*, 35−41.
(54) Gust, D.; Moore, T. A.; Moore, A. L. Molecular Mimicry of Photosynthetic Energy and Electron Transfer. *Acc. Chem. Res.* **1993**, *26*, 198−205.
(55) Gust, D.; Moore, T. A.; Moore, A. L. Mimicking Photosynthetic Solar Energy Transduction. *Acc. Chem. Res.* **2001**, *34*, 40−48.
(56) Straight, S. D.; Liddell, P. A.; Terazono, Y.; Moore, T. A.; Moore, A. L.; Gust, D. All-Photonic Molecular XOR and NOR Logic Gates Based on Photochemical Control of Fluorescence in a Fulgimide-Porphyrin-Dithienylethene Triad. *Adv. Funct. Mater.* **2007**, *17*, 777−785.

(57) Straight, S. D.; Kodis, G.; Terazono, Y.; Hambourger, M.; Moore, T. A.; Moore, A. L.; Gust, D. Self-Regulation of Photoinduced Electron Transfer by a Molecular Nonlinear Transducer. *Nat. Nanotechnol.* **2008**, *3*, 280−283.
(58) Terazono, Y.; Kodis, G.; Bhushan, K.; Zaks, J.; Madden, C.; Moore, A. L.; Moore, T. A.; Fleming, G. R.; Gust, D. Mimicking the Role of the Antenna in Photosynthetic Photoprotection. *J. Am. Chem. Soc.* **2011**, *133*, 2916−2922.